

# Spatially Resolved Detection of Attomole Quantities of Organic Molecules Localized in Picoliter Vials Using Time-of-Flight Secondary Ion Mass Spectrometry

Robert M. Braun,<sup>†</sup> Arthur Beyder,<sup>‡</sup> Jiyun Xu, Mark C. Wood,<sup>§</sup> Andrew G. Ewing,<sup>||</sup> and Nicholas Winograd\*

Department of Chemistry, The Pennsylvania State University, 184 Materials Research Institute Building, University Park, Pennsylvania 16802, and Department of Chemistry, The Pennsylvania State University, 152 Davey Laboratory, University Park, Pennsylvania 16802

**Time-of-flight secondary ion mass spectrometry (TOF-SIMS) has been utilized to detect femtomole and attomole quantities of organic species from within silicon nanovials. By using high-density arrays (10 000 nanovials/cm<sup>2</sup>) it is possible to chemically characterize diverse sample sets within a single chemical image. Molecular sensitivities, for the compounds investigated, vary between 85 attomoles and 25 femtomoles, and typical acquisition times are approximately 100 ms per nanovial. These vials are fabricated using photolithography and KOH etching of Si{001} wafers to create wells, with a pyramidal cross section, ranging in size from 25 to 5625 μm<sup>2</sup>. The volume ranges from 30 femtoliters to 100 picoliters, respectively. A drawn glass microinjector and solenoid-driven dispenser are utilized to array picoliter volumes of organic compounds into individual silicon nanovials. Solution concentrations typically range from 1 × 10<sup>-2</sup> to 1 × 10<sup>-4</sup> M allowing femtomole and even attomole quantities of material to be dispensed into each vial.**

Miniaturization concepts have recently been brought to the forefront of the analytical sciences. This paradigm shift toward micro- and nanoscale experiments is driven partly by increasing chemical and waste removal costs, but mostly by the constantly improving sensitivity of modern analytical equipment. Moreover, instrumental acquisition time often plays a critical role in the overall throughput of a given technique. Presently, there are numerous laboratories that utilize some form of parallel synthetic processes to create new chemical entities.<sup>1,2</sup> This powerful,

synthetic methodology allows chemically diverse sample sets (i.e., libraries) to be created in order to facilitate the discovery of new materials, catalysts, and even pharmaceutical agents.<sup>3,4</sup> Most importantly, the speed at which these compounds and materials are generated dictates the need for new analytical techniques and protocols that are better able to process samples in a parallel manner.

Recently, there have been numerous reports describing the fabrication of sample substrates that contain an array of subnanoliter reservoirs on a single chip. The fabrication methods include microcontact printing,<sup>5</sup> glass etching,<sup>6</sup> pressure imprinting,<sup>7</sup> laser ablation,<sup>8</sup> and photolithography.<sup>9–11</sup> Although no one method has proven to be superior, photolithography offers tremendous versatility and is often the method of choice. Specifically, nanovials, etched into the surface of silicon wafers, have been used to hold pico- to nanoliter volumes of liquid. In some cases lithographically made silicon templates have been used to imprint nanovials into polymers.<sup>12</sup> These wells are subsequently used to perform a variety of experiments including volume-limited voltammetry,<sup>12,13</sup> capillary electrophoresis from extremely small volumes,<sup>14,15</sup> biotin/aequorin binding assays,<sup>16</sup> and even oligonucleotide and DNA product

\* Corresponding author: (tel.) 814-863-0001; (fax) 814-863-8081; (e-mail) nxw@psu.edu.

<sup>†</sup> Present Address: Blacklight Power, Inc., East Windsor, NJ 08520.

<sup>‡</sup> Present Address: SUNY at Buffalo, Amherst, NY 14226

<sup>§</sup> Present Address: United States Army Research Laboratory, Adelphi, MD 20783.

<sup>||</sup> Department of Chemistry, The Pennsylvania State University, 152 Davey Laboratory.

(1) For a review and applications of parallel synthetic techniques see the entire volume of *Chem. Rev.* **1997**, 97.

(2) For a review of recent concepts involving combinatorial chemistry and sample processing see the entire volume of *Nature (London)* **1996**, 384 supp.

(3) Xiang, X. D.; Sun, X.; Briceno, G.; Lou, Y.; Wang, K. A.; Chang, H.; Wallace-Freedman, W. G.; Chen, S. W.; Schultz, P. G. *Science (Washington, D.C.)* **1995**, 268, 1738–1740.

(4) Thompson, L. A.; Ellman, J. E. *Chem. Rev.* **1996**, 96, 555–600.

(5) Grzybowski, B. A.; Haag, R.; Bowden, N.; Whitesides, G. M. *Anal. Chem.* **1998**, 70, 4645–4652.

(6) Michael, K. L.; Taylor, L. C.; Schultz, S. L.; Walt, D. R. *Anal. Chem.* **1998**, 70, 1242–1248.

(7) Martynova, L.; Locascio, L. E.; Gaitan, M.; Kramer, G. W.; Christensen, R. G.; MacCrehan, W. A. *Anal. Chem.* **1997**, 69, 4783–4789.

(8) Roberts, M. A.; Rossier, J. S.; Bercier, P.; Girault, H. *Anal. Chem.* **1997**, 69, 2035–2042.

(9) Haginoya, C.; Ishibashi, M.; Koike, K. *Appl. Phys. Lett.* **1997**, 71, 2934–2936.

(10) Jansson, M.; Emmer, A.; Roeraade, J.; Lindberg, U.; Hok, B. *J. Chromatogr.* **1992**, 626, 310–314.

(11) Jespersen, S.; Niessen, W. M. A.; Tjaden, U. R.; van der Greef, J.; Litborn, E.; Lindberg, U.; Roeraade, J. In *Mass Spectrometry in the Biological Sciences*; Burlingame, A. L., Carr, S. A., Eds.; Humana Press: Totowa, NJ, 1996; pp 217–226.

(12) Clark, R. A.; Hietpas, P. B.; Ewing, A. G. *Anal. Chem.* **1997**, 69, 259–263.

(13) Clark, R. A.; Ewing, A. G. *Anal. Chem.* **1998**, 70, 1119–1125.

(14) Hietpas, P. B.; Ewing, A. G. *J. Liq. Chromatogr.* **1995**, 18, 3557–3576.

identification.<sup>17</sup> Although impressive detection limits down to attomoles for the bioluminescence assays have been achieved, none of these techniques has proven to be a high-throughput characterization tool. However, recent matrix assisted laser desorption ionization (MALDI) experiments performed on synthetic oligonucleotides show promise in the high-throughput arena.<sup>17</sup> In the example presented, 8 fmol of an oligonucleotide was added to each 800  $\mu\text{m} \times 800 \mu\text{m}$  vial in a 100-well (12-mm) array. The acquisition time for the 100 nanovial set was 43 min, a time which could be reduced even further with refinements in the software.

In our laboratory we have designed and fabricated a substrate that can hold 10 000 samples within a 1.4  $\text{cm}^2$  silicon chip. More importantly, we have utilized the chemical imaging capabilities of time-of-flight secondary ion mass spectrometry (TOF-SIMS) to help alleviate the characterization bottleneck discussed above. In this paper, we show that it is possible to rapidly isolate subpicomole quantities of material within arrays of nanovials etched into the surface of a silicon wafer. A finely focused ion beam is used to desorb ions from within each nanovial, and the ejected ions are subsequently extracted into a TOF mass analyzer. By accurately recording the mass spectral information as a function of ion beam position it is possible to create a chemical map or image of the nanovial array with typical acquisition times of  $\leq 100$  ms per well. We show several examples that illustrate the high sensitivity of this technique as well as how it can be applied as a high-throughput characterization tool for materials analysis and drug development within the pharmaceutical industry.

## EXPERIMENTAL SECTION

**Reagents.** The Si{001} wafers were purchased from Silicon Quest International (Santa Clara, CA) and were coated with 1000  $\text{\AA}$  of  $\text{Si}_3\text{N}_4$  at the National Nanofabrication Facility (Cornell, NY) prior to etching. The crystal violet, melatonin, and uridine samples were purchased from Sigma-Aldrich (Milwaukee, WI) and were used without purification. Ultrahigh-purity water was purchased from VWR (Pittsburgh, PA) and utilized as a solvent or cosolvent during the delivery process. Ethanol (dehydrated, 200-proof) was purchased from Pharmco Products (Brookfield, CT) and was also used as a solvent or cosolvent.

**Micropipet Fabrication and Liquid Delivery.** Pipets were pulled using a Sutter Instrument Company (Navato, CA) Model P-97 micropipette puller. Two different capillary sizes were chosen to deliver a wide range of liquid volumes which correspond to the nanovial size range given below. Specifically, glass capillaries from A-M Systems Incorporated (Everett, WA; P/N 6020, 1.2-mm o. d., 0.68-mm i. d.) were used to handle relatively large volumes, while smaller volumes were delivered using capillaries from Sutter Instrument Co. (P/N B100-75-10, 1.0-mm o. d., 0.75-mm i. d.). After the pipets were pulled, roughly 25% of the pipets within a given batch were chosen at random to calibrate the delivery characteristics.

Once selected, each pipet was back-loaded with an appropriate solution using a microfil syringe needle (World Precision Instruments, Sarasota, FL). Once loaded, the nontapered end of the pipet was connected to a General Valve Picospritzer (Fairfax, NJ) which allowed precise control of the delivered volume from the tapered end of the pipet by simply adjusting the pressure and pulse width of a pneumatic solenoid. Delivery was accomplished by directly contacting the end of the pipet with the center of the nanovial. Volume calibration of the pipets was accomplished by injecting a small volume of liquid into a pool of silicone oil or glycerol. By retaining the oil on a glass microscope slide, it was possible to utilize a gradicule and accompanying light microscope to measure the diameter of the injected liquid. Simple calculations revealed the volume contained within the sphere. Using this approach, we were able to reproducibly deliver liquids in the range of  $40 \pm 15$  to  $425 \pm 35$   $\mu\text{L}$  for the large pipets and  $1.0 \pm 0.5$  to  $64 \pm 12$   $\mu\text{L}$  using the smaller diameter pipets. Finally, each pipet was discarded after about 10–15 delivery cycles ( $\sim 50$  nanovials) to prevent tip clogging due to the high surface area to volume ratio of liquid present in the pipet tip.

**Nanovial and Sample Substrate Fabrication.** The {001} surface of silicon was chosen because of the convergent self-limiting  $\langle 111 \rangle$  etch planes that are  $54.74^\circ$  from the (001) surface of the wafer, thus allowing nanovials with a pyramidal cross section to be created.<sup>10,18</sup> The nanovial arrays were fabricated on a Si{001} wafer using photolithographic techniques and a newly designed chromium-on-glass mask. Prior to processing, 1000  $\text{\AA}$  of  $\text{Si}_3\text{N}_4$  was deposited on the undoped Si{001} surface by the National Nanofabrication Facility. The nitride surface was then coated with Shipley's 1813 photoresist, exposed to UV light in a Karl Suss MA-6 photolithography instrument, and developed using MF-312 developer. This process transferred the nanovial pattern (arrays) to the 3-in. OD wafers. The nitride was removed using a  $\text{CF}_4/\text{O}_2$  plasma, and the remaining photoresist was then stripped using acetone and 2-propanol. Anisotropic etching along the  $\langle 110 \rangle$  directions was performed using a 40% (w/w) potassium hydroxide in water solution. This procedure resulted in vials with a well-defined geometry, therefore facilitating the determination of the internal volume using a Tencor Instruments stylus profilometer and scanning electron microscope (SEM).

A cross-sectional view of a single nanovial is shown in Figure 1A. This scanning electron micrograph clearly illustrates the flat bottom and tapered walls of the vials. Each nanovial has a pyramidal cross section, and the sizes range from 25 to 5625  $\mu\text{m}^2$  which corresponds to a volume range of 30 femtoliters to 100 picoliters, respectively. A top view of a small portion of the arrayed nanovials is shown in Figure 1B. The corners of four  $20 \times 20$  nanovial arrays are shown in this SEM image.

Last, this particular vial shape was chosen because of the varying surface angles established by the {001} and {111} facets. It is known that large ion beam incidence angles, with respect to the surface normal, increase secondary-ion yields from most substrates.<sup>19,20</sup> Consequently, we created a surface with compound angles so the secondary-ion yield would be enhanced from the sides and bottom of the vials using an ion beam with a  $50^\circ$

(15) Hietpas, P. B.; Gilman, D.; Lee, R. A.; Wood, M. C.; Winograd, N.; Ewing, A. G. In *Nanofabrication and Biosystems: Integrating Materials Science, Engineering and Biology*; Hoch, H. H., Jelinski, L. W., Craighead, H., Eds; Cambridge University Press: NY, 1996; pp 139–158.

(16) Crofcheck, C. L.; Grosvenor, A. L.; Anderson, K. W.; Lumpp, J. K.; Scott, D. L.; Daunert, S. *Anal. Chem.* **1997**, *69*, 4768–4772.

(17) Little, D. P.; Cornish, T. J.; O'Donnell, M. J.; Braun, A.; Cotter, R. J.; Koster, H. *Anal. Chem.* **1997**, *69*, 4540–4546.

(18) Barycka, I.; Zubeł, I. *Sens. Actuators, A* **1995**, *48*, 229–238.

(19) Winograd, N. *Prog. Solid State Chem.* **1982**, *13*, 285–375.

(20) Xu, C.; Burnham, J. S.; Braun, R. M.; Goss, S. H.; Winograd, N. *Phys. Rev. B: Condens. Matter* **1995**, *52*, 5172–5178.

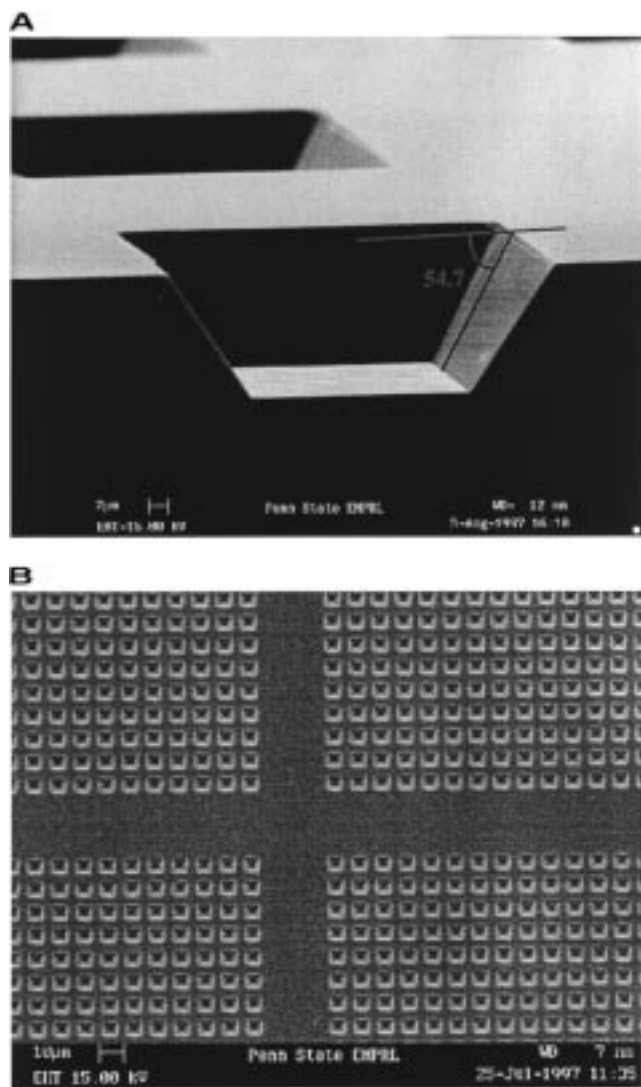


Figure 1. Shown are two scanning electron microscopy images of nanovials which have been etched into the surface of a Si{001} wafer. Image A is a cross-sectional view of a  $50\ \mu\text{m} \times 50\ \mu\text{m}$  nanovial showing the tapered walls and flat bottom. The lower image (B) shows the intersection of four  $20 \times 20$  arrays (top view). A thermal intensity scale is employed where white represents the maximum count rate and black represents the minimum count rate.

incidence angle. In contrast, when the ion beam incidence angle is nearly parallel to the surface, a decrease in secondary-ion intensity is expected. These concepts are further illustrated below.

**Mass Spectrometer.** The TOF-SIMS instrumentation has been described in detail elsewhere and will be briefly discussed below.<sup>21,22</sup> A 25 keV liquid metal ( $\text{Ga}^+$ ) ion gun with a beam current of 1 namp and a pulse length of 10 ns is used to desorb ions from the uppermost layers of a sample within an ultrahigh vacuum environment. By rastering this finely focussed ( $<200\ \text{nm}$ ), pulsed ion beam across a surface, it is possible to rapidly collect an entire mass spectrum at each point (i.e., pixel) within the rastered field. The system can acquire up to 10 000 mass spectra/

(21) Braun, R. M.; Blenkinsopp, P.; Mullock, S. J.; Corlett, C.; Willey, K. F.; Vickerman, J. C.; Winograd, N. *Rapid Commun. Mass Spectrom.* **1998**, *12*, 1246–1252.

(22) Willey, K. F.; Vorsa, V.; Braun, R. M.; Winograd, N. *Rapid Commun. Mass Spectrom.* **1998**, *12*, 1253–1260.

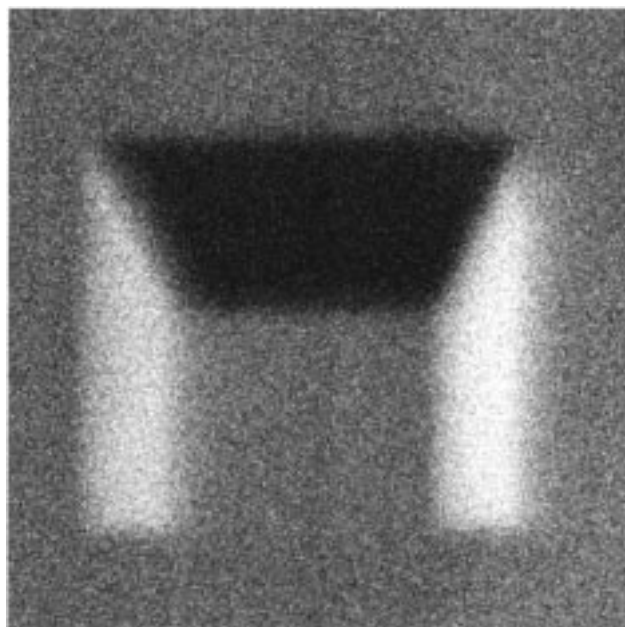


Figure 2. The  $\text{Si}^+$  ion intensity as a function of ion beam position across a single nanovial ( $256 \times 256$  pixels). The secondary-ion intensity clearly varies as a function of the ion beam incidence angle along each facet within this  $64\ \mu\text{m} \times 64\ \mu\text{m}$  field of view. The shape of the nanovial helps increase secondary-ion yields and ultimately improves detection limits.

s. The individual mass spectra (pixels) are then summed as a function of  $x$  and  $y$  position of the ion beam, yielding a chemical map of the sample surface. The resulting image provides chemically and spatially resolved information about the surface composition at the micrometer level. Computer control of the instrument allows for relatively easy identification of chemically diverse samples, since all mass spectral information is stored for future reference. Furthermore, TOF-SIMS is a rather nondestructive technique, since 1% or less of a monolayer is typically consumed during an experiment.<sup>23</sup> This low consumption is accomplished by keeping the incident ion dose at or below  $5 \times 10^{12}$  ions/ $\text{cm}^2$  (20 repetitions/pixel) and is often referred to as the static limit.

## RESULTS AND DISCUSSION

**TOF-SIMS Characterization of Nanovials.** As mentioned previously, the nanovial shape was chosen because of enhanced secondary-ion yields expected from the tapered surfaces. The goal is to improve the detection limits using TOF-SIMS by tailoring the physical characteristics of the substrate. An example of increased secondary-ion yield from an empty silicon nanovial is illustrated in Figure 2. Shown is the  $\text{Si}^+$  ion intensity as a function of ion beam position across the vial. The ion beam is incident along the bottom of the image at an angle of  $50^\circ$  to the silicon surface, and the bottom edge (facet) of the nanovial is not clearly defined because the ion beam is nearly parallel to this surface. In contrast, the top facet of the vial presents a surface that is nearly normal to the ion beam, and the resulting  $\text{Si}^+$  ion intensity is between the secondary ion yields from the bottom edge and the sides of the vial. More interestingly, the right and left facets of

(23) Benninghoven, A. *Angew. Chem., Int. Ed. Engl.* **1994**, *33*, 1023–1043.

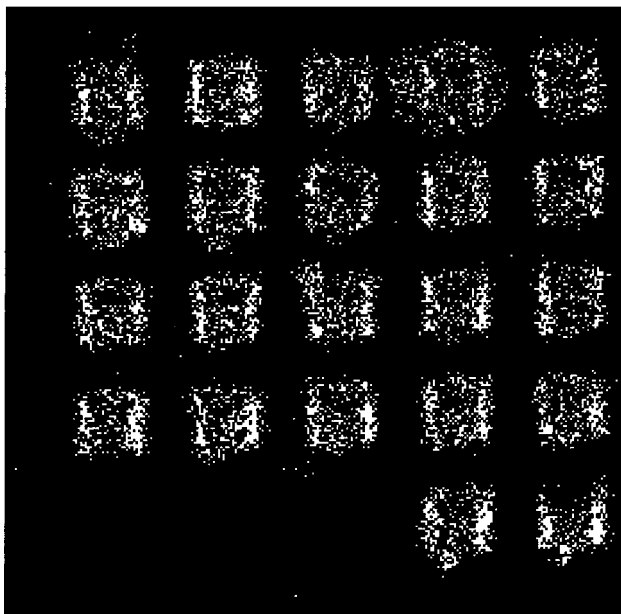


Figure 3. Crystal violet (500 fmol) injected into 50  $\mu\text{m}$  nanovials. The  $(\text{M} + \text{H})^+$  ion intensity of crystal violet is plotted as a function of lateral position within this 490  $\mu\text{m} \times 490 \mu\text{m}$  image (256  $\times$  256 pixels). Each point represents a single count. Each vial was loaded individually except for the vials in the lower left portion of the image, which were not loaded and, consequently, used as blanks.

the nanovial account for slightly over 52% of the  $\text{Si}^+$  ion intensity arising from within the well. The far edge and bottom account for approximately 17.5 and 30.2%, respectively.

To validate the use of TOF-SIMS as a high-throughput characterization tool, we analyzed several samples loaded into 50  $\mu\text{m} \times 50 \mu\text{m}$  vials. The images clearly show how subpicomole quantities of material can be efficiently localized within the vials, and the corresponding signal intensities indicate the rather low detection limits offered by TOF-SIMS. All compounds were loaded into individual nanovials using the pipets and picospritzer discussed above.

Crystal violet, which is an antimicrobial agent and biological stain, was chosen as a model to investigate the delivery and localization of molecules inside individual nanovials. This molecule has also been successfully detected previously in a similar environment.<sup>15</sup> A 15% (v/v) solution of ethanol and water worked best to dissolve the crystal violet and promote good wetting characteristics along the bottom and sides of the nanovials. Each nanovial shown in Figure 3 was loaded with 500 fmol of crystal violet and clearly illustrates how the molecules are localized to the wells. Signal intensities for the  $(\text{M} + \text{H})^+$  ion averaged  $300 \pm 18$  counts per nanovial using an incident ion dose of  $3.6 \times 10^{10}$  ions/ $\text{cm}^2$ , and the acquisition time was 65 ms per nanovial which is a significant improvement over existing mass spectral techniques. The vials in the lower left portion of the image were not filled and, thus, were used as blanks.

At present, we have limited the image sizes to illustrate the versatility and practicality of using TOF-SIMS imaging to characterize large sample sets. However, the present limitation is strictly based on the manual nature of the delivery system. Ultimately, the spectrometer images over an area of 4 mm  $\times$  4 mm. Using the current nanovial substrates, a 16 mm<sup>2</sup> image contains 1600 (50  $\mu\text{m}$ ) nanovials corresponding to a total acquisi-

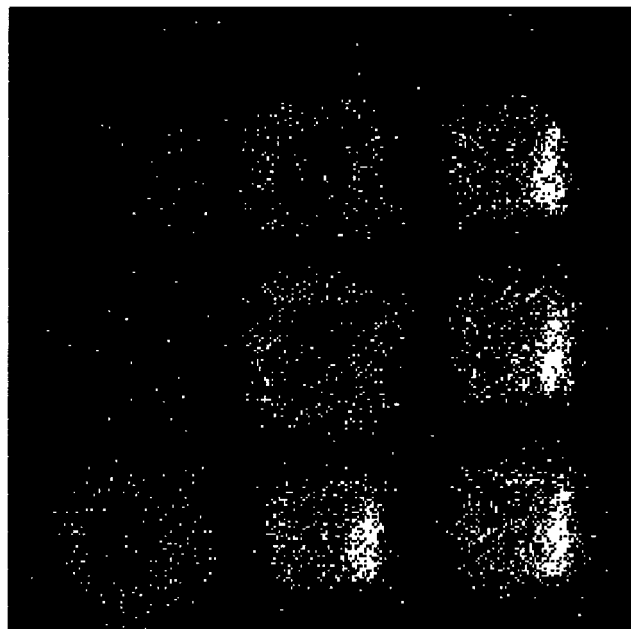


Figure 4. Concentration gradient of crystal violet injected into a series of nanovials. The amount of crystal violet varies from 18 fmol (lower right vial) to 85 amol (upper left vial) within this 322  $\mu\text{m} \times 322 \mu\text{m}$  image (256  $\times$  256 pixels), and the results establish a relative detection limit for this molecule. The specific amounts are 18 fmol, 12 fmol, 6 fmol, 3 fmol, 1.2 fmol, 600 amol, 580 amol, 290 amol, and 85 amol, respectively.

tion time of 1.7 min, or 65 ms per nanovial. In comparison, acquisition times for LC-MS, NMR, and ESI-MS experiments are typically greater than 5 min per sample which results in an acquisition time of  $\geq 130$  h for the same 1600 sample set. Consequently, TOF-SIMS imaging offers the ability to significantly reduce data acquisition times while working with very small quantities of material.

The relative sensitivity level for crystal violet within the silicon nanovials is illustrated in Figure 4. The concentration of molecules within each vial was varied from  $18.0 \pm 2.0$  fmol to  $85 \pm 50$  amol. Even though each nanovial contains trace levels of compound, it is possible to isolate the crystal violet to the wells, as well as to obtain reasonably strong  $(\text{M} + \text{H})^+$  ion intensity from each well. Specifically, the ion intensity varies from over 500 counts to slightly over 15 counts per nanovial, respectively, using an incident ion dose of  $1.4 \times 10^{11}$  ions/ $\text{cm}^2$ .

For comparison, an image obtained from a binary system consisting of melatonin and uridine is shown in Figure 5. This 500  $\mu\text{m} \times 500 \mu\text{m}$  image shows alternating columns of melatonin (red) and uridine (green) while the  $\text{Si}^+$  ion intensity from the underlying substrate is shown in blue. Each nanovial in the array was filled with  $2.4 \pm 0.7$  pmol of the respective compound, and the resulting  $(\text{M} + \text{H})^+$  ion intensity (pixels) from each well is shown in the image. The incident ion dose was  $8.5 \times 10^{10}$  Ga<sup>+</sup> ions per  $\text{cm}^2$ , which is well below the damage threshold defined by the static SIMS regime. Even at this low incident ion dose, the molecular ion intensity from within each nanovial clearly shows how the compounds are isolated to these small defined environments. The average  $(\text{M} + \text{H})^+$  ion intensity from the melatonin and uridine vials is  $221 \pm 27$  and  $192 \pm 19$  counts, respectively. Furthermore, by extending the incident Ga<sup>+</sup> ion dose

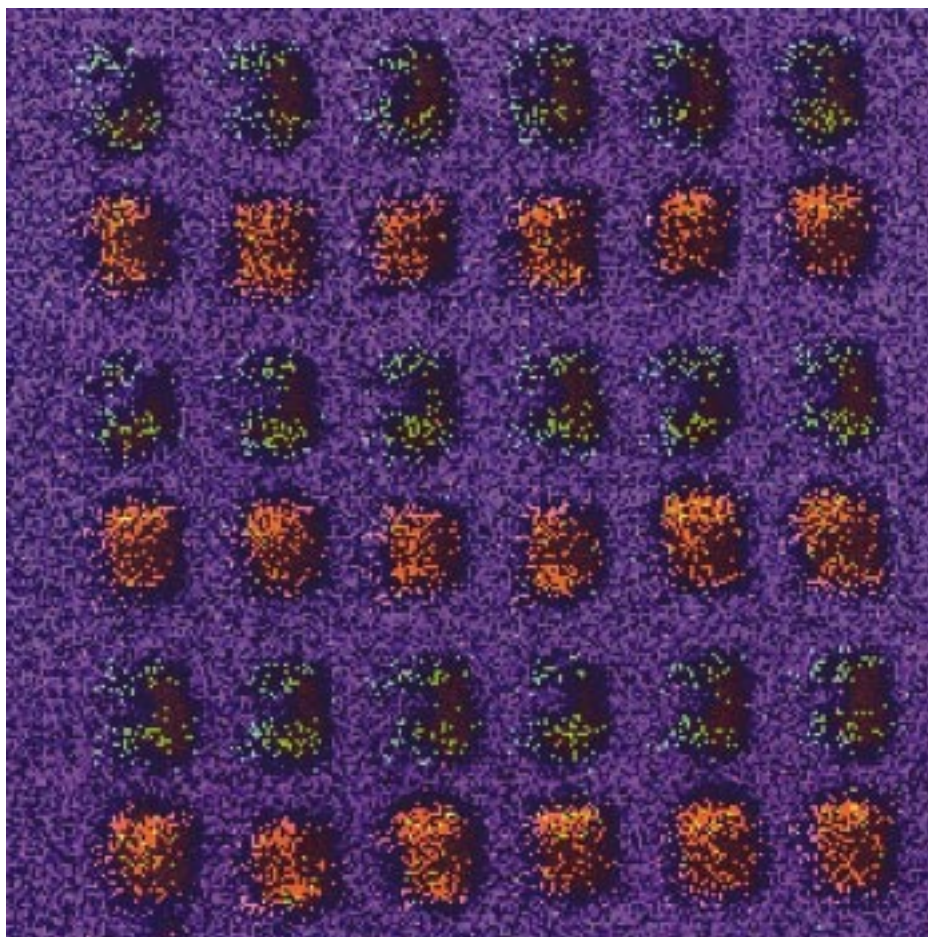


Figure 5. Binary array of melatonin and uridine. Each nanovial was loaded with 2.4 pmol of the respective molecules. The alternating array is established starting with melatonin (red) in the right column and finishing with uridine (green) in the left column. The  $(M + H)^+$  secondary ion intensity is shown as a function of ion-beam position within a  $500 \mu\text{m} \times 500 \mu\text{m}$  field of view.

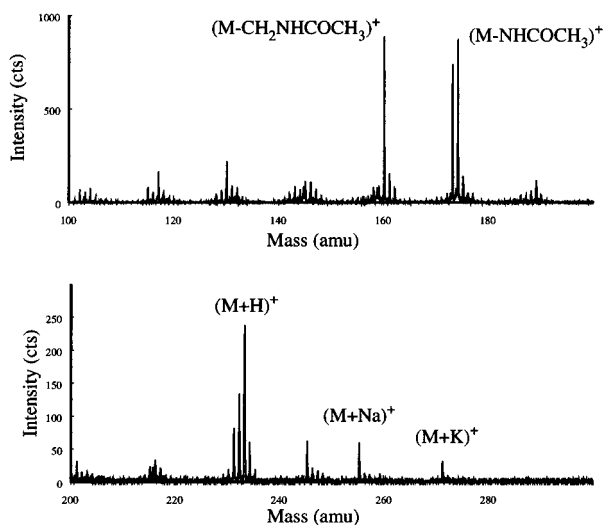


Figure 6. Representative mass spectrum obtained from 2.4 pmol of melatonin localized within a single  $50 \mu\text{m}$  nanovial. The molecular ion  $(M + H)^+$ , as well as structurally significant fragment ions, are clearly observed within the spectrum.

to  $4 \times 10^{12}$  ions/cm<sup>2</sup> (static limit), the  $(M + H)^+$  ion intensity increases to approximately 6900 counts for the same 2.4-pmol quantities. A mass spectrum of melatonin desorbed from a single nanovial loaded with 2.4 pmol is shown in Figure 6. At the 2-pmol

level, we clearly have adequate signal-to-noise ratios and are able to accurately identify the peaks within the spectrum.

By combining high sensitivity and large field imaging, it is possible to illustrate further the usefulness of TOF-SIMS imaging when applied to large arrays. A  $930 \mu\text{m} \times 930 \mu\text{m}$  image ( $10 \times 11$  vials) of melatonin ( $24 \pm 7$  fmol/vial) is shown in Figure 7. Once again, the  $(M + H)^+$  ion intensity is shown superimposed over the  $\text{Si}^+$  ion intensity desorbed from the substrate. The average melatonin signal is  $22 \pm 6$  counts per vial, using an incident  $\text{Ga}^+$  ion dose of  $5.1 \times 10^{10}$  ions/cm<sup>2</sup>. Although it would be difficult to perform bioassays and observe enzyme and inhibitor binding reactions using femtomole quantities of material, the examples above clearly demonstrate the ability to characterize large numbers of samples within a single chemical image.

One important parameter that must be addressed when working with very small volumes of liquid ( $<1$  nL) is solvent evaporation. Typically, the solvent evaporates in less than one second during the delivery of about 1 pL to the vial. In recent electrochemical experiments,<sup>12,13</sup> performed within individual nanovials, water evaporation was abated by addition of glycerol to the matrix within the nanovial. In addition, an evaporation block system has been used by placing a layer of octane over the aqueous-filled nanovials.<sup>24</sup> Although both of these options are fine choices when dealing with biologically related systems, we believe

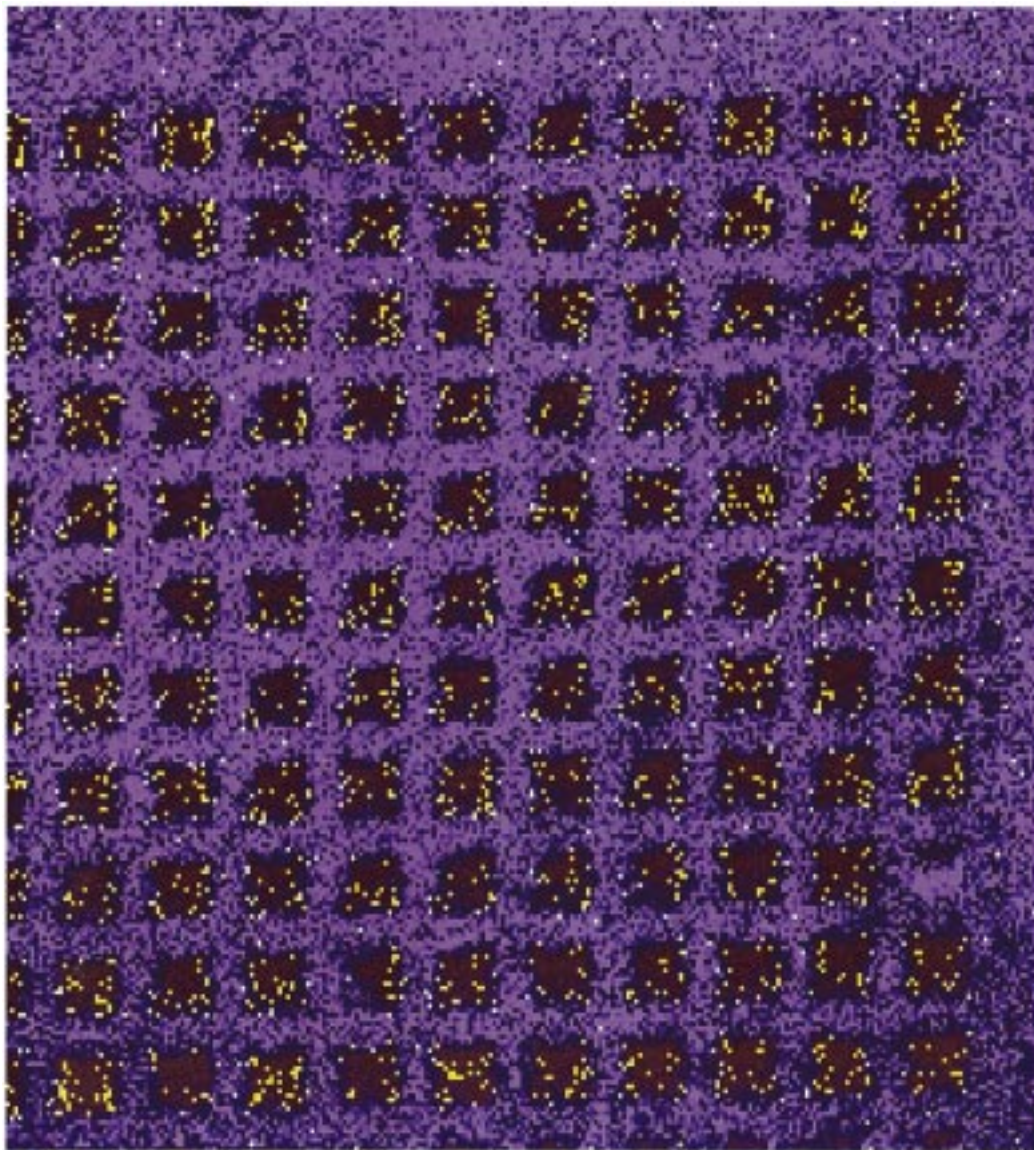


Figure 7. A  $930\ \mu\text{m} \times 930\ \mu\text{m}$   $(\text{M} + \text{H})^+$  ion image ( $256 \times 256$  pixels) of melatonin ( $24 \pm 7$  fmol) injected into a  $10 \times 11$  array of  $50\ \mu\text{m}$  nanovials. The implications of high-throughput characterization are detailed in the text.

it is better to choose a solvent or solvent mixture that yields the best wetting properties within the nanovials when performing TOF-SIMS experiments. This option proves to be the simplest because it limits the amount of processing equipment and allows sample handling to be performed in an ambient environment. Moreover, by improving solvent wetting, the sample surface area and overall exposure of the molecules to the ion beam is maximized. During these investigations, however, we have not yet attempted to modify the surface of the silicon wafers to help tailor their wetting properties.

**Future Directions.** Clearly, to fully exploit TOF-SIMS imaging as a high-throughput technique, we require a parallel-loading mechanism to insert a diverse set of molecules into the nanovials. In particular, we are currently working on ways to improve the picospritzer design to develop a parallel-loading strategy which will allow for more efficient loading and processing of the

nanovials, as well as allowing for larger arrays ( $>100$  wells/image) to be easily addressed. At present, there are several commercially available dispensing technologies. One involves the use of inkjets<sup>25</sup> to deliver liquid pulses to a substrate. Unfortunately, the jets are prone to clogging and are difficult to clean once a liquid is dispensed. In addition, it is very difficult to accurately deliver subnanoliter volumes using ink jets. Second, syringe pumps have been used to deliver nanoliter volumes onto a variety of substrates.<sup>26</sup> This technology has significant ramifications in the pharmaceutical industry and is directly adaptable to our needs by simply increasing the nanovial dimensions. Currently, the industry standard substrate is a 96-well ( $\sim 3 \times 5$  in.) titer plate. Our goal is to reformat these 96-well plates into a higher density package such as the silicon wafers described above.

(25) For a detailed explanation of ink-jet technology and delivery systems contact Microdrop GmbH. (Norderstedt, Germany) and Microfab Technologies, Inc. (Plano, TX).

(26) For a complete description of liquid-handling technology on the nL scale contact Cartesian Technologies (Irvine, CA).

(24) Litborn, E.; Stjernstrom, M.; Roeraade, R. *HPCE Abstract*, 1998, Orlando FL, pp 205; abstract P432.

## CONCLUSIONS

High-density nanovial arrays have been fabricated in silicon wafers allowing 10 000 samples per 1.4 cm<sup>2</sup> to be neatly indexed. This type of arraying technology is shown to be an excellent strategy to isolate large numbers of femtomole and attomole quantities of material on a single substrate. When the sample sets are characterized using TOF-SIMS imaging, it is possible to accurately record the mass spectrum of the material within each nanovial. Moreover, the speed with which these measurements are performed indicates that TOF-SIMS can routinely characterize samples in a high-throughput fashion. This tremendous improvement in acquisition time ( $\leq 100$  ms/vial) far exceeds the current performance specifications of NMR, LC-MS, MALDI, and ESI-MS techniques. Once a parallel-loading strategy is incorporated into the liquid delivery system, TOF-SIMS imaging is poised to

become a routine processing tool within the parallel (combinatorial chemistry) synthesis arena.

## ACKNOWLEDGMENT

The authors wish to thank R. Clark and D. Cannon for many helpful discussions and for sharing their expertise involving the fabrication of micro-pipets. The authors would also like to thank M. Rogosky for his help with the photolithographic processes required during the nanovial production. Last, we would like to thank the National Institutes of Health and the National Science Foundation for financial assistance.

Received for review February 22, 1999. Accepted May 18, 1999.

AC9902042